International Journal of Horticultural Science and Technology

Journal homepage: https://ijhst.ut.ac.ir

Assessment of Spring Frost Tolerance in Almond Cultivars and Genotypes Using Thermal Analysis

Ali Kasraeian[1], Ali Tehranifar[1]*, Ali Imani[2], Yahya Selahvarzi[1]

1 Department of Horticultural Science and Landscape Architecture, Ferdowsi University of Mashhad, Mashhad, Iran

2 Temperate Fruit Research Center, Horticultural Research Institute, Agricultural Research, Education and Extension Organization (AREEO), Karaj, Iran

ARTICLE INFO

*Corresponding author's email: tehranifar@um.ac.ir

ABSTRACT

The blossoming of almond trees often overlaps with spring frosts, posing a significant risk of reduced or even nullified yields. However, almonds exhibit genetic variability in their response to extreme cold and frost. Identifying frost-resistant cultivars and genotypes through reliable evaluation methods and leveraging their genetic potential is a promising strategy to mitigate spring frost damage. This study explored the response of various almond cultivars and genotypes to frost damage using controlled freezing and thermal analysis. Two experiments were conducted separately in 2019 and 2020. The first experiment employed thermal analysis to evaluate the frost tolerance of six almond genotypes (S1, S2, A5, A8, A11, and A23) across three phenological stages: green tip, popcorn, and open flower. The second experiment examined the frost tolerance of 26 cultivars/genotypes in 2019 and 30 in 2020 at the open flower stage. This was achieved through a combination of thermal analysis, visual inspection, and ion leakage assessment in a controlled temperature chamber. The findings revealed that both the phenological stage and the specific cultivars/genotypes significantly influenced the exotherm temperature of almond flower buds. A positive correlation was observed between the exotherm temperature of flower and leaf buds, frost damage, and ion leakage, highlighting the practicality of thermal analysis as a tool for assessing frost tolerance in almonds. Based on the results of thermal analysis, cultivars/genotypes D12, Saba, KD101, KD99, A5, and C16 were identified as leading candidates for future almond breeding programs.

Introduction

Low-temperature injury significantly limits fruit crop production, particularly for temperate fruit trees (Kang et al., 1998; Yu and Lee, 2020). Consequently, efforts to maximize production and mitigate losses due to low temperatures have focused on implementing freeze-protection methods and selecting cold-resistant cultivars (Kang et al., 1998). The ability of deciduous fruit trees to tolerate spring frost largely depends on their genotype. Genetically controlled traits such as flower super-cooling capacity, blooming time, flower bud density, and the uniformity of bud development significantly influence flower survival during frosts (Rodrigo, 2000).

Almonds are especially vulnerable to spring frosts due to their early flowering. In most almond-growing regions, the buds, flowers, and developing fruits are susceptible to damage after

breaking dormancy (Imani and Mahamadkhani, 2011). The expansion of almond cultivation into areas where spring frost coincides with bloom has further increased the risk of reduced or even nullified yields (Socias i Company and Gradziel, 2017). While breeding efforts have achieved progress in developing late-blooming cultivars, this approach alone is insufficient to fully address spring frost damage. Therefore, enhancing frost hardness is also a key objective in almond breeding programs (Imani and Mahamadkhani, 2011; Socias i Company and Gradziel, 2017).

Studies have revealed significant genetic variability in the response of almond cultivars and genotypes to very low temperatures and frost (Imani et al., 2011; Imani et al., 2012; Socias i Company and Gradziel, 2017). A fast and accurate method for differentiating cultivars and genotypes based on their cold tolerance is essential (Nazemi et al., 2016). Various methods have been used to assess frost damage in temperate fruit trees, both in the field and laboratory. These include visual inspection of frost damage, thermal analysis, ion leakage, and triphenyl tetrazolium chloride (TTC) reduction analysis (Yu and Lee, 2020). Among these, visual inspection and ion leakage are the most frequently used techniques for evaluating the cold tolerance of almond flower buds (Bigdeli Moheb et al., 2018; Imani et al., 2011; Socias i Company and Gradziel, 2017). However, while these methods detect plant tissue death caused by exposure to freezing temperatures, they do not clearly identify the temperature thresholds at which tissue death occurs (Kaya et al., 2018).

Thermal analysis, on the other hand, can quickly detect supercooling capacity in temperate fruit trees during controlled freezing tests. This method measures the latent heat of fusion, including high-temperature exotherms (HTE) and low-temperature exotherms (LTE), which correspond to the crystallization of extracellular and intracellular supercooled water, respectively, using thermoelectric modules in laboratory-based freezing assays (Faust, 1989; Kaya and Kose, 2019). Previous studies have documented HTE and LTE in the dormant buds of deciduous fruit species, such as grapevine (Mills et al., 2006), walnut (Aslamarz et al., 2010), apricot (Ashworth et al., 1981), peach (Liu et al., 2019), and sweet cherry (Salazar-Gutiérrez et al., 2014). However, after bud dormancy is broken, thermal analysis in flower buds of many *Prunus* and other deciduous species often detects a single-peaked exotherm (Kaya et al., 2020; Kaya et al., 2018). This single exotherm suggests simultaneous freezing in intracellular and extracellular compartments, indicating a lethal temperature (Kaya and Kose, 2019; Malyshev et al., 2020).

Determining the supercooling threshold and evaluating the spring frost tolerance of almond buds through thermal analysis will deepen our understanding of almond frost hardiness and enhance the effective utilization of genetic resources. The primary objective of this study is to evaluate whether thermal analysis can reliably assess the frost tolerance of almond flower buds across various genotypes and cultivars. Additional goals include investigating the spring frost tolerance of flower buds, identifying the supercooling threshold, and examining the relationship between exotherms, visual inspection, and ion leakage.

Material and methods
Plant materials
The almond cultivars and genotypes used in this study were grown in an experimental orchard at the Horticultural Research Station in Karaj, Alborz province, Iran (35°45'N, 50°57'E, 1250 m elevation). The trees, aged 8–10 years, were managed under uniform cultural practices, including irrigation and fertilization.

This study consisted of two separate experiments conducted in 2019 and 2020. The first experiment evaluated six almond genotypes (S1, S2, A5, A8, A11, and A23) across three phenological stages: green tip, popcorn, and open flower. The second experiment assessed 26 genotypes and cultivars in 2019 and 30 in 2020, focusing on the open flower stage.

For each experiment, three shoots (20–25 cm long) containing flower buds were collected from various sides of each tree. The shoots were placed in plastic bottles filled with water and promptly transported to the laboratory for analysis.

Exotherm analysis
The method used in this study followed the protocols previously described by Quamme (1974), Salazar-Gutiérrez et al. (2014), and Yu and Lee (2020). Thermal analysis was conducted using a programmable freezer and a multi-channel data logger equipped with DS18B20 temperature sensors (Maxim IC, USA). The sensors were attached to intact buds using elastic bands to ensure secure contact. The samples were wrapped with thermal insulation foam and aluminum foil to minimize heat loss and were placed in Dewar flasks pre-chilled to 5 °C. These flasks were then positioned in a freezing chamber programmed to cool at a rate of 2 °C h^{-1}. The freezing process began at 5 °C and continued until the chamber temperature reached -20 °C. The use

of Dewar flasks helped to minimize temporal temperature fluctuations within the chamber, maintaining a consistent cooling rate of approximately 1.8 °C h⁻¹.

Bud temperatures were monitored at 20-s intervals using the data logger. Exotherms, characterized by sudden temperature deflections, were identified as the buds began to freeze. These temperature deflections occur when the latent heat of moisture content within the buds is released during freezing, producing curves on the temperature-time graph known as exotherms. The specific temperature at which freezing occurs is referred to as the exotherm temperature. To analyze the data, the time-temperature area under the curve (AUC) for temperatures above the exotherm temperature was calculated using OriginPro 2019b (OriginLab Corporation, Northampton, MA, USA). Figure 1 illustrates this process.
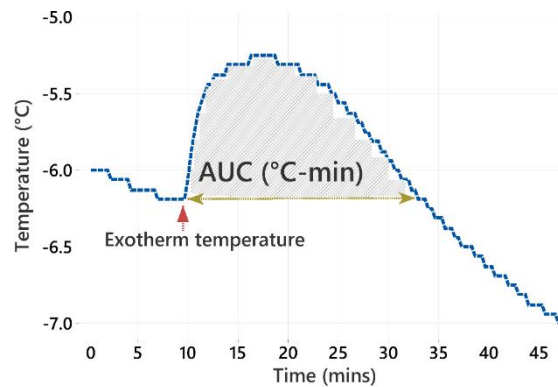

Fig. 1. Exotherm temperature and the area under the curve (AUC) on the time-temperature graph.

Fresh weight and moisture content

The buds were collected from the shoots, immediately weighed with precision (0.0001 g) (fresh weight), placed in an oven at 70 °C for 2 d, and weighed again (dry weight). The moisture content of the buds was determined as a percentage of the fresh weight using the following formula:

$$\text{Moisture content} = [\frac{(\text{Fresh weight} - \text{Dry weight})}{\text{Fresh weight}}] \times 100$$

Cold treatment and frost damage

A controlled-temperature chamber was utilized to conduct cold treatment. The chamber was programmed to decrease the temperature gradually at 2 °C h⁻¹. The cooling process began at 7 °C and continued until the temperature reached -3.5 °C. The samples were kept at -3.5 °C for 60 min, after which the temperature was gradually increased at 2 °C h⁻¹ until it reached 7 °C again. After the cold treatment, the stems were kept at ambient conditions for 24 h. The flowers were examined using a stereomicroscope, and the extent of frost damage was evaluated based on the degree of discoloration and browning (Bigdeli Moheb et al., 2018; Miranda et al., 2005; Pakkish and Tabatabaienia, 2016).

Ion leakage

Ion leakage was measured using a method similar to that described in the literature (Barranco et al., 2005). After the cold treatment, the flowers were excised (about 0.5 g) and washed with distilled water. Next, the samples were transferred into tubes containing 15 ml of distilled water. The tubes were then shaken continuously at 120 rpm for 24 h at room temperature (24 °C ± 1). The electrical conductivity (EC) of the first solution was measured using an EC-meter and recorded as EC1. Then, the tubes were autoclaved at 120 °C at 1 atm for 1 h. The tubes were subsequently shaken for an additional 2 h at 200 rpm at room temperature, and EC was measured again and recorded as EC2. Finally, the ion leakage was calculated based on the relative electrical conductivity (ECr) using the following formula:

$$\text{ECr} = (\frac{EC1}{EC2}) \times 100$$

Statistical analysis

This study consisted of two separate experiments. The first examined six almond genotypes at three phenological stages using a factorial arrangement, based on a completely randomized design with three replications. In the second experiment, we investigated the genotypes and cultivars at the open-flower stage

with three replications using a completely randomized design. The data were analyzed using Minitab 21. Mean values were compared using Tukey's HSD test ($P \leq 0.05$), and correlation analysis was performed using Pearson's correlation coefficient.

Results
This study comprised two separate experiments, each conducted in duplicate during 2019 and 2020. For the first experiment, the results from the second replication in 2020 were consistent with those from the first replication in 2019.

Therefore, only the 2019 results will be presented for this experiment. In contrast, for the second experiment, the results from both replications (2019 and 2020) will be reported, as the cultivars/genotypes differed between the two years.

Results of the first experiment
The ANOVA results for exotherm temperature, AUC, fresh weight, and moisture content indicated that genotypes and phenological stages significantly influenced all the parameters ($P < 0.01$) (Table 1).

Table 1. ANOVA (mean squares) of the exotherm temperature (ET), area under the curve (AUC), fresh weight (FW), and moisture content (MC) of flower buds from six almond genotypes at three phenological stages.

Sources of Variance	DF	Mean squares			
		ET	AUC	FW	MC
Genotype	5	18.674**	1376.61**	11187.3**	14.761**
Phenological stage	2	13.527**	3332.97**	43552.5**	97.045**
Genotype*Phenological stage	10	4.632**	117.03**	969.3**	2.538**
Error	36	0.223	19.38	11.6	0.1530

**Significance ($P < 0.01$).

Thermal analysis and exotherm temperature
A single distinct exotherm was observed in the time-temperature profiles of almond flower buds at each phenological stage (green tip, popcorn, and open flower) within the temperature range of 5 °C to -20 °C (Fig. 2). The exotherm temperature of the flower buds was significantly influenced by both phenological stage and genotype. Among the phenological stages, the highest exotherm temperature (-6.3 °C) was recorded at the green tip stage, which was significantly higher than that at the popcorn stage. Conversely, the lowest exotherm temperature (-7.97 °C) was associated with the popcorn stage, which did not significantly differ from the open flower stage (Fig. 3, left).
Regarding genotypes, the lowest exotherm temperature (-10.14 °C) was observed in A5, significantly lower than all other genotypes. In contrast, the highest exotherm temperature (-6.1 °C) was recorded in A23, which was not significantly different from S1, S2, A8, and A11 (Fig. 3, right). The interaction between genotype and phenological stage also influenced the exotherm temperature, with values ranging from -5.21 °C (A23 at the green tip stage) to -12.27 °C (A5 at the popcorn stage). A23 exhibited the highest exotherm temperatures across all phenological stages (-5.21 °C at green tip, -6.81 °C, at popcorn, and -6.35 °C, at open flower). In contrast, S2 recorded the lowest exotherm temperature at the green tip stage (-6.77 °C),

while A5 showed the lowest exotherm temperatures at the popcorn (-12.27 °C) and open flower (-11.81 °C) stages (Fig. 4).

Area under the curve (AUC)
The AUC of the flower buds was significantly influenced by the phenological stage, genotype, and their interaction. Among the phenological stages, the minimum AUC (16.78 °C-min) was observed during the green tip stage, which was significantly different from the popcorn and open-flower ones. On the other hand, the maximum AUC (42.25 °C-min) was obtained during the open flower stage, which was not significantly different from the popcorn one (Fig. 5 left). Regarding the genotypes, the maximum AUC belonged to S1 and S2 (49.31 and 46.14 °C-min, respectively). At the same time, A23 had the lowest AUC (19.40 °C-min) and had no significant differences with A5, A8, and A11 (Fig. 5 right). Due to the interaction of the phenological stage and genotype, the AUC values ranged from 6.61 °C-min for A23 at the green tip stage to 69.79 °C-min for S1 at the open-flower stage. During the green tip and open flower stages, S1 had the highest AUC (26.04 and 69.79 °C-min, respectively), while S2 had the highest AUC (57.04 °C-min) at the popcorn stage. In contrast, A23 had the lowest AUC for all three stages, with 6.61, 25.34, and 26.25 °C-min for the green tip, popcorn, and open-flower stages, respectively (Fig. 6).
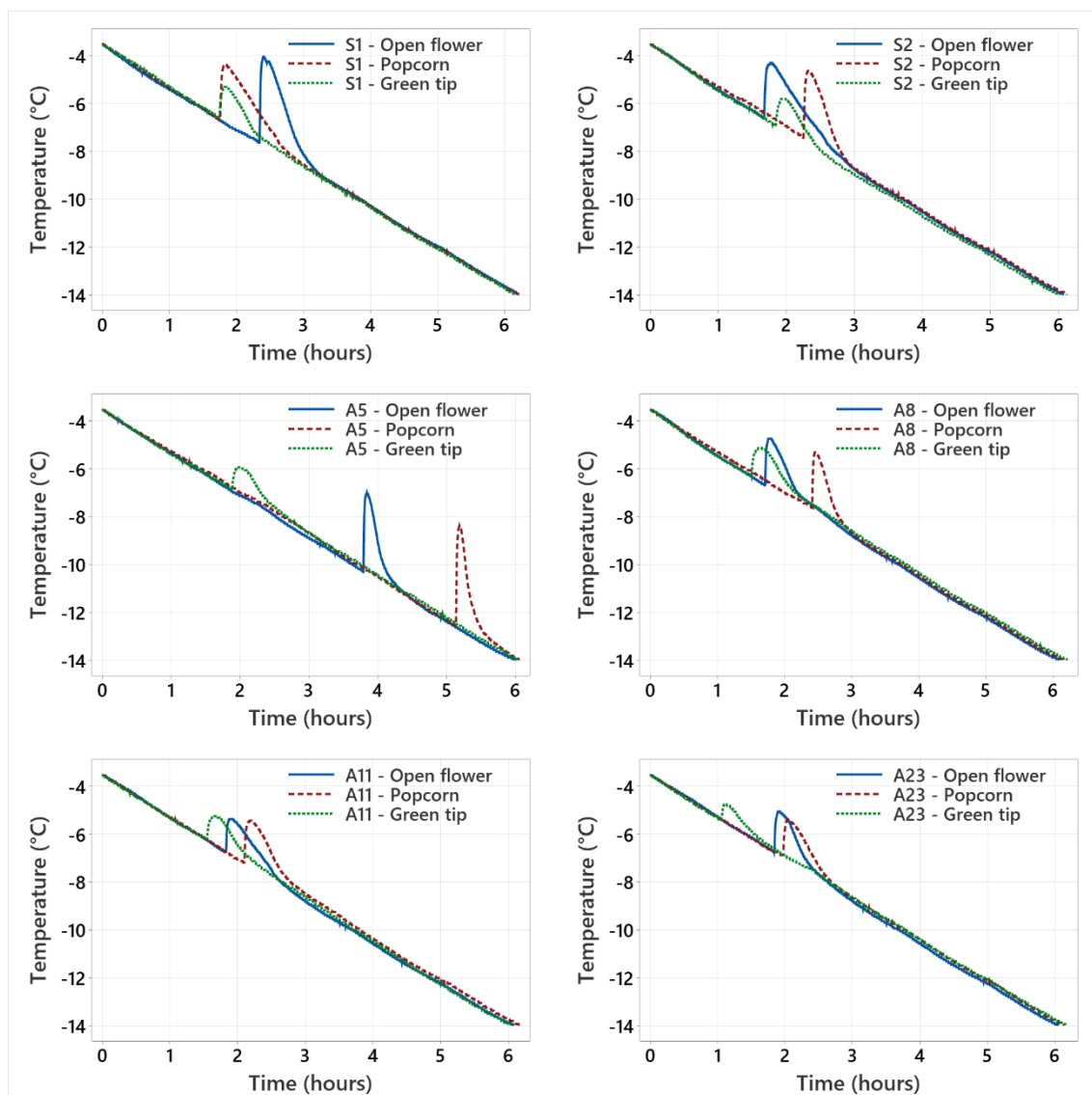
Fig. 2. Thermal analysis of flower buds from six almond genotypes (S1, S2, A5, A8, A11, and A23) at three phenological stages (green tip, popcorn, and open flower).
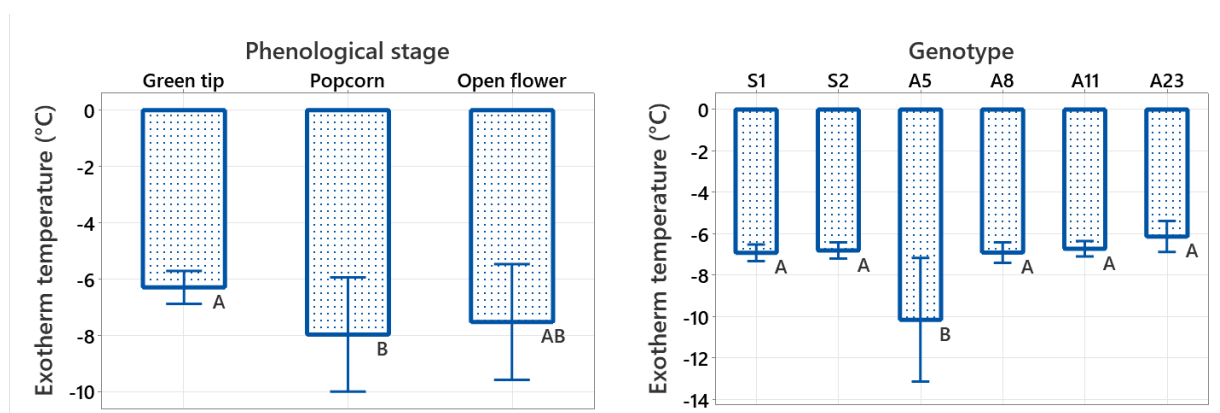

Fig. 3. Exotherm temperature of flower buds at three phenological stages (left) and six almond genotypes (right). Vertical bars denote the standard deviation (SD) of mean values. Mean values that share the same letter indicate non-significant differences ($P \leq 0.05$).
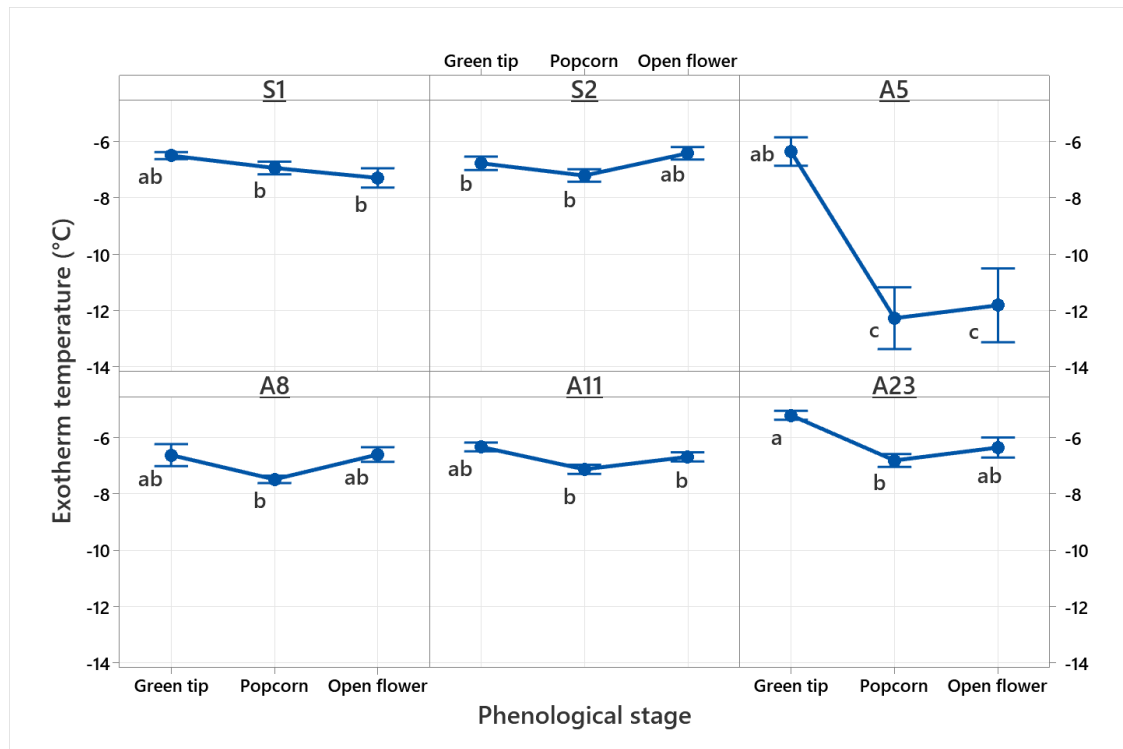
Fig. 4. Interactive effect of phenological stage (green tip, popcorn, and open flower) and genotype (S1, S2, A5, A8, A11, and A23) on the exotherm temperature of almond flower buds. Vertical bars represent standard deviation (SD) of mean values. Mean values that share the same letter indicate non-significant differences ($P \leq 0.05$).
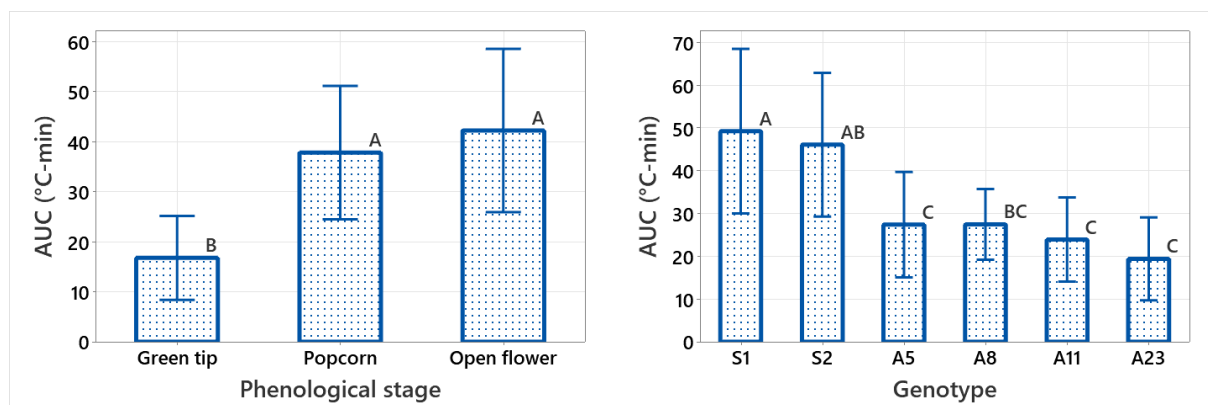

Fig. 5. The area under the curve (AUC) of the flower bud exotherm at three phenological stages (left) and six almond genotypes (right). Vertical bars exhibit the standard deviation (SD) of mean values. Mean values that share the same letter indicate non-significant differences ($P \leq 0.05$).

Fresh weight of flower buds

As the phenological stage progressed, the fresh weight of the flower buds increased. The open flower stage exhibited the highest fresh weight (223.3 mg per flower bud (FB^{-1}), significantly higher than the green tip and popcorn stages. Conversely, the lowest fresh weight (126.2 mg FB^{-1}) was observed at the green tip stage, which was significantly different from the other stages (Fig. 7, left). Among the genotypes, S1 and S2 recorded the highest fresh weights, with values of 238.9 mg FB^{-1} and 201.7 mg FB^{-1}, respectively. In contrast, A23 had the lowest fresh weight (142.6 mg FB^{-1}), which was significantly different from S1 (Fig. 7, right). Across the green tip, popcorn, and open flower stages, S1 consistently displayed the highest fresh weights, measuring 163.19, 262.97, and 290.75 mg FB^{-1}, respectively. In comparison, A23 consistently recorded the lowest fresh weights for all three stages, with values of 109.04, 159.34, and 159.46 mg FB^{-1}, respectively (Fig. 8).
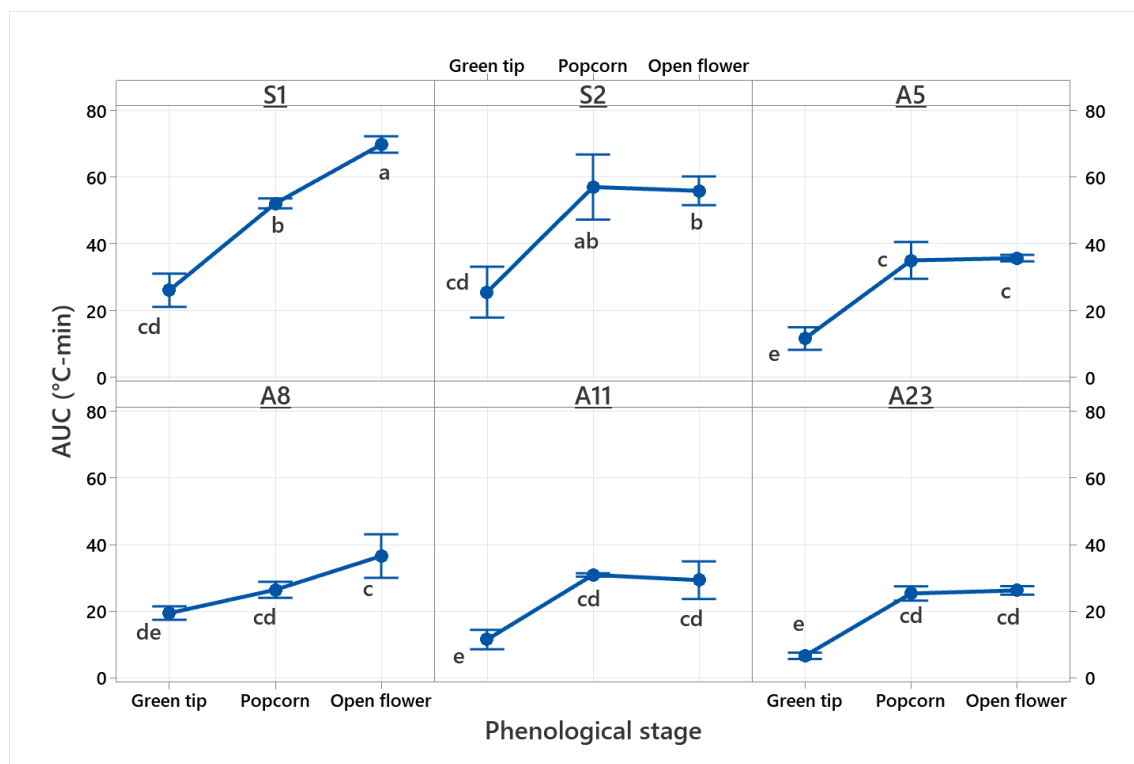
Fig. 6. The interactive effect of phenological stage (green tip, popcorn, and open flower) and genotype (S1, S2, A5, A8, A11, and A23) on the area under the curve (AUC) of the almond flower bud exotherm. Vertical bars show the standard deviation (SD) of mean values. Mean values that share the same letter indicate non-significant differences ($P \leq 0.05$).
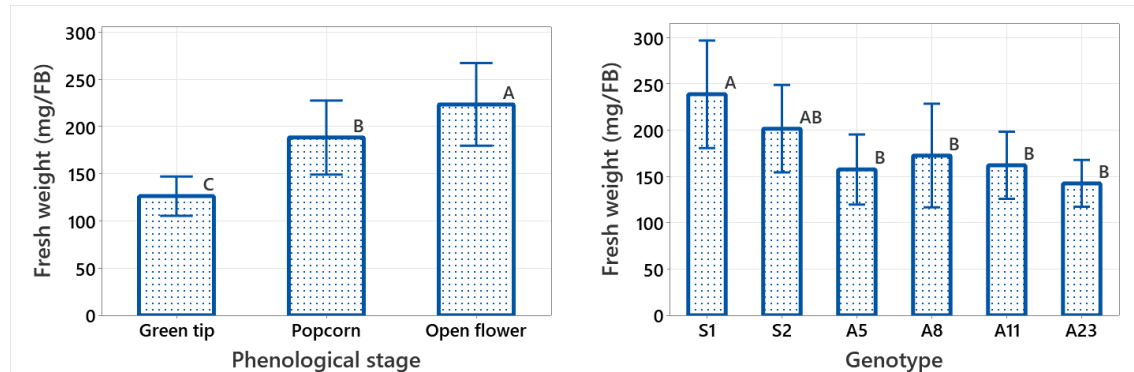

Fig. 7. Fresh weight of flower buds at three phenological stages (left) and six almond genotypes (right). Vertical bars are the standard deviation (SD) of means. Means that share the same letter indicate non-significant differences ($P \leq$ 0.05).

Moisture content of flower buds

Significant differences in the moisture content of flower buds were observed across phenological stages and among genotypes. As the flower buds developed, their moisture content increased. The highest moisture content (81.06%) was recorded at the open flower stage, which did not significantly differ from the popcorn stage. In contrast, the lowest moisture content (76.63%) was observed at the green tip stage, significantly lower than that of the popcorn and open flower stages (Fig. 9, left). Among the genotypes, A8 and A5 exhibited the highest moisture contents, with 80.51% and 80.28%, respectively. In contrast, A11 had the lowest moisture content (77.34%), significantly differing from A8 (Fig. 9, right). At specific phenological stages, the maximum moisture contents were 77.71%, 82.2%, and 82.47% for S2 at the green tip stage, A8 at the popcorn stage, and A5 at the open flower stage, respectively. Conversely, the lowest moisture contents were observed in A11 at the green tip (75.62%) and open-flower (78.06%) stages, and in A23 at the popcorn stage (78.05%) (Fig. 10).
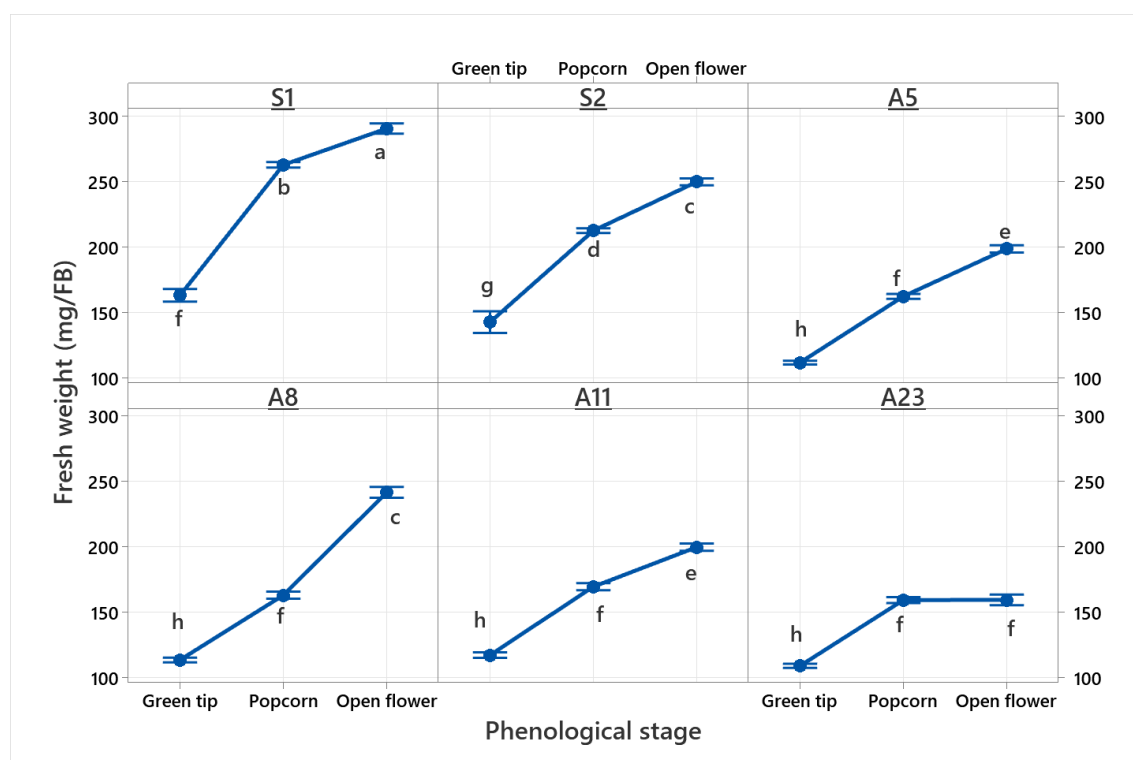
Fig. 8. The interactive effect of phenological stage (green tip, popcorn, and open flower) and genotype (S1, S2, A5, A8, A11, and A23) on fresh weight of almond flower buds. Vertical bars represent the standard deviation (SD) of means. Means that share the same letter indicate non-significant differences ($P \leq 0.05$).
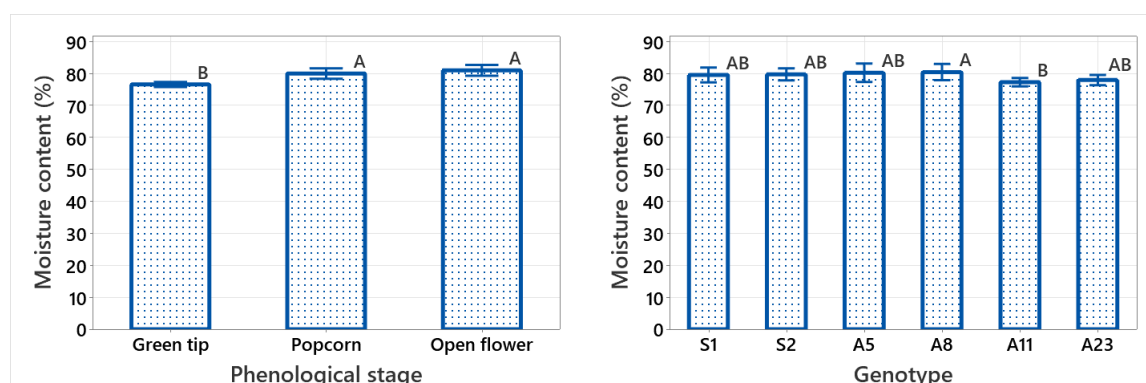

Fig. 9. Moisture content of flower buds at three phenological stages (left) and six almond genotypes (right). Vertical bars denote the standard deviation (SD) of means. Means that share the same letter indicate non-significant differences ($P \leq 0.05$).

Correlations between the variables of the first experiment

The results of our study revealed a strong positive correlation between the area under the curve (AUC) and the fresh weight of flower buds ($r = 0.924$, $p < 0.001$). Additionally, a moderate correlation was observed between the AUC and the moisture content of the flower buds ($r = 0.693$, $p = 0.001$). As expected, there was also a significant correlation between the moisture content and fresh weight of the flower buds ($r = 0.714$, $p = 0.001$). However, no significant correlations were found between the bud exotherm temperature and either of the fresh weight or the AUC (Fig. 11).

Results of the second experiment

ANOVA results indicated that genotypes significantly influenced all parameters in 2019-2020, including flower bud exotherm temperature, leaf bud exotherm temperature, frost damage, and ion leakage ($P < 0.01$) (Table 2).
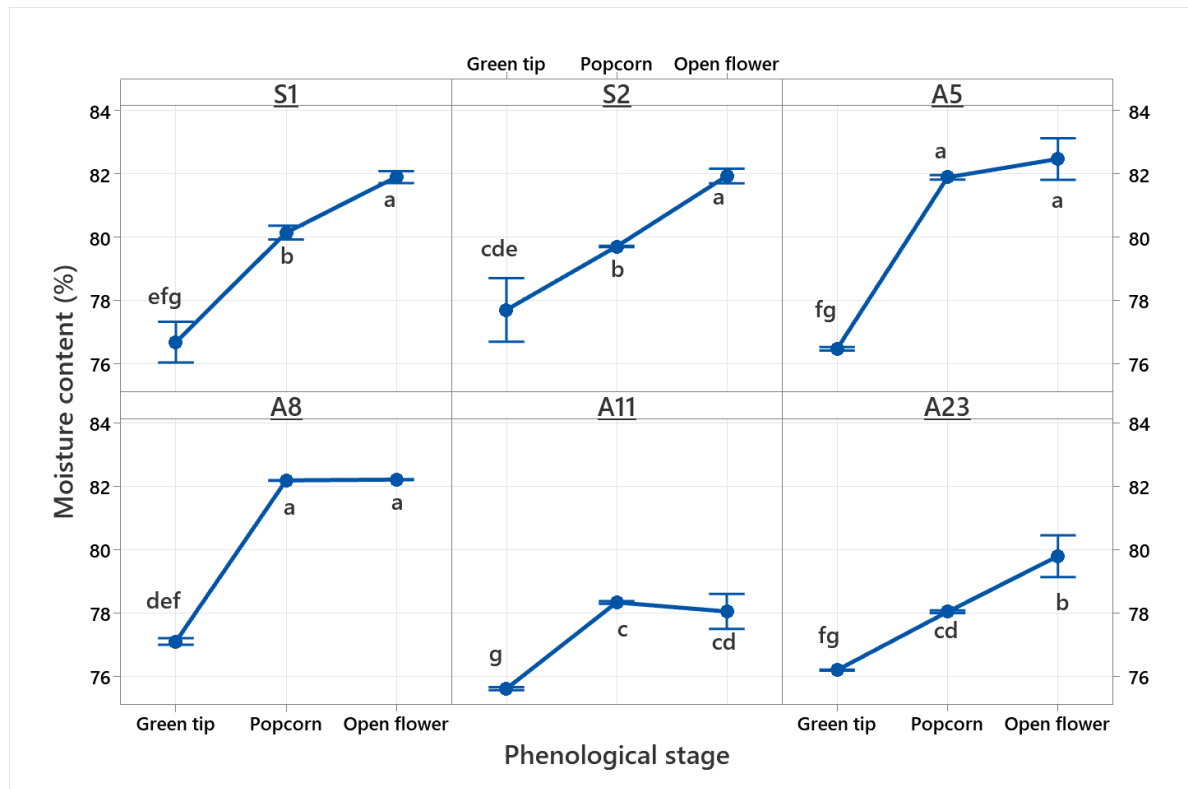
Fig. 10. The interactive effect of phenological stage (green tip, popcorn, and open flower) and genotype (S1, S2, A5, A8, A11, and A23) on the moisture content of the almond flower buds. Vertical bars are the standard deviation (SD) of means. Means that share the same letter indicate non-significant differences ($P \leq 0.05$).
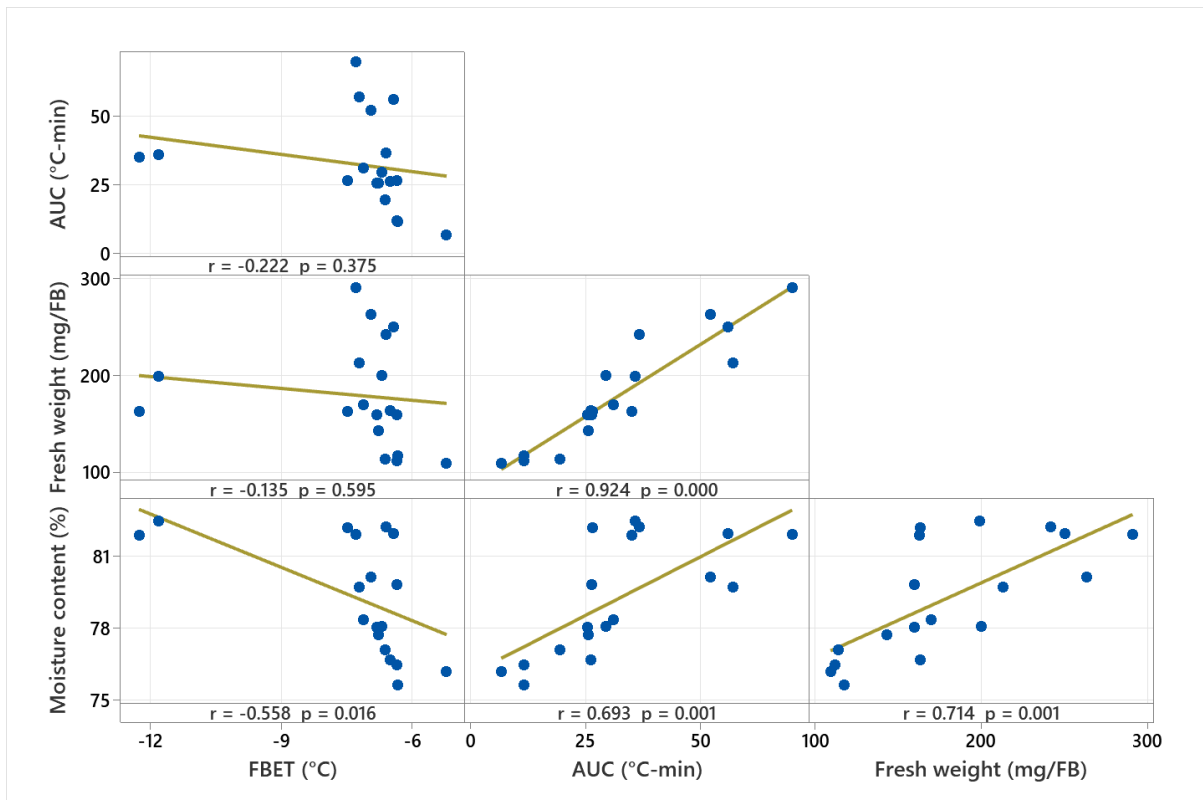

Fig. 11. Matrix plot of the correlations between the flower bud exotherm temperature (FBET), area under the curve (AUC), fresh weight, and moisture content of the almond flower buds (r: Pearson's correlation coefficient, n = 18).

Exotherm temperature of flower buds

In 2019, the flower buds of D12 exhibited the lowest exotherm temperature (-12.69 °C). Following D12, A5 (-11.81 °C) and C16 (-10.67 °C) had the second and third lowest exotherm temperatures, respectively. Conversely, the highest exotherm temperature (-5.83 °C) was observed in A25, which was not significantly different from A21, A23, A8, A11, S2, C9, MS9, MS7, C5, MS3, and Golqermez (Fig. 12). In 2020,

D12 (-12.41 °C) had the lowest exotherm temperature, followed by Saba (-11.94 °C), KD101 (-11.87 °C), C16 (-11.12 °C), A5 (-11.10 °C), and KD99 (-10.87 °C). These cultivars/genotypes exhibited significant differences compared to the others. On the other hand, Marcona recorded the highest exotherm temperature (-5.48 °C), which was not significantly different from those of K9-7, KD1-16, A23, A11, A8, and Sahand (Fig. 13).

Table 2. ANOVA (mean squares) of the flower bud exotherm temperature (FBET), leaf bud exotherm temperature (LBET), frost damage (FD), and ion leakage (IL) from almond buds sampled in 2019-2020.

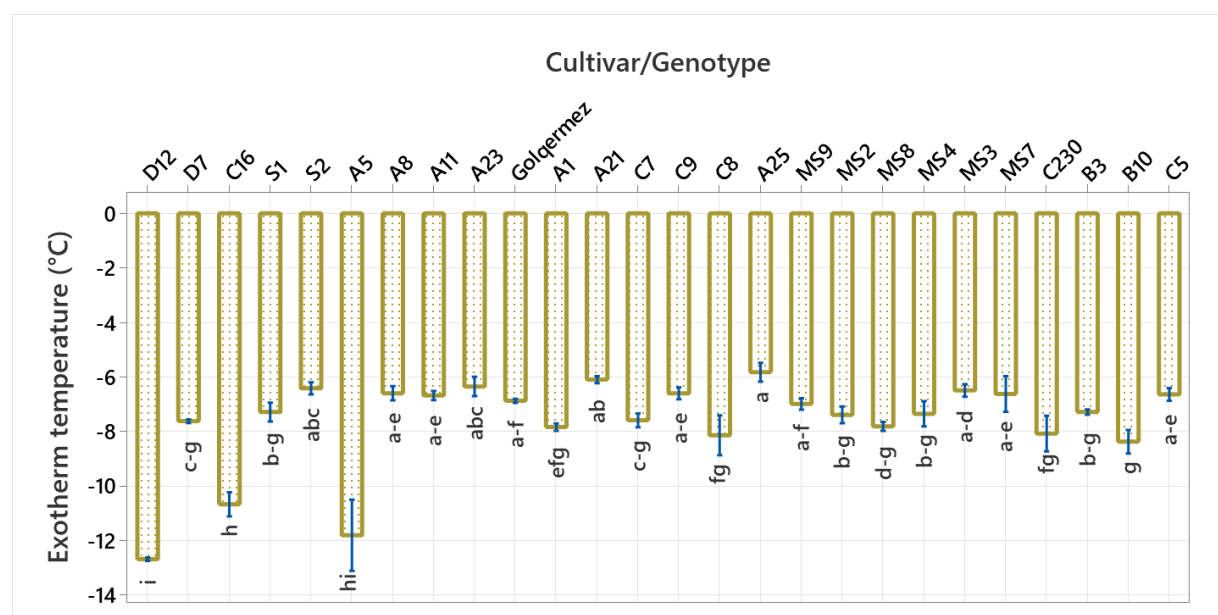| Sources of Variance (2019)	DF	Mean squares			
		FBET	LBET	FD	IL
Cultivar/Genotype	25	8.371**	3.961**	789.07**	58.367**
Error	52	0.178	0.122	41.13	5.849
Sources of Variance (2020)	DF	Mean squares			
		FBET	LBET	FD	IL
Cultivar/Genotype	29	11.240**	5.154**	799.39**	119.151**
Error	60	0.170	0.182	38.16	5.841

**Significance ($P < 0.01$).

Fig. 12. Exotherm temperature of almond flower buds sampled at the open flower stage in 2019. Vertical bars show the standard deviation (SD) of means. Means that share the same letter indicate non-significant differences ($P \leq$ 0.05).

Exotherm temperature of leaf buds

The genotype significantly influenced the exotherm temperature of the leaf buds. In 2019, the lowest exotherm temperatures were recorded for A5 (-9.70 °C), D12 (-9.54 °C), and C16 (-9.52 °C). In 2020, the lowest temperatures were observed in Saba (-11.43 °C), KD101 (-11.04 °C), A5 (-10.50 °C), KD99 (-9.77 °C), D12 (-

9.35 °C), and C16 (-9.27 °C). On the other hand, the highest exotherm temperatures in 2019 were observed in MS3 (-5.50 °C), A23 (-5.66 °C), C5 (-5.70 °C), A25 (-6.15 °C), A21 (-6.20 °C), and C9 (-6.29 °C). In 2020, A23, Sahand, A11, and A8 recorded the highest exotherm temperatures at -6.37, -6.37, -6.60, and -6.60 °C, respectively (Figs. 14 and 15).
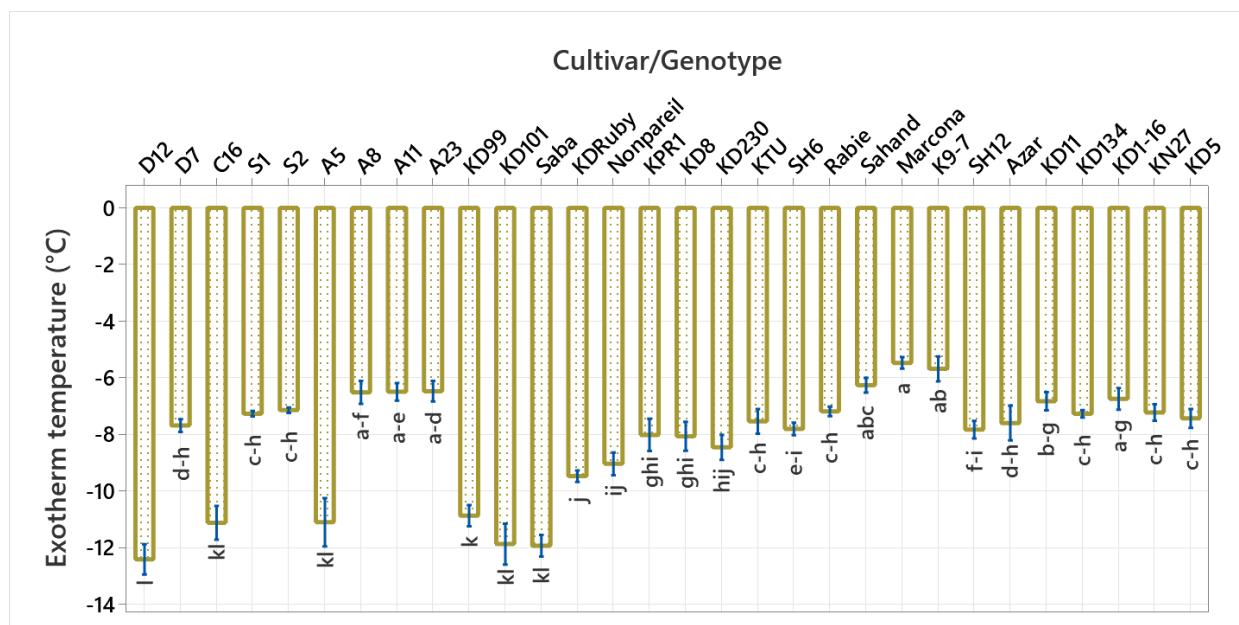
Fig. 13. Exotherm temperature of almond flower buds sampled at the open flower stage in 2020. Vertical bars demonstrate the standard deviation (SD) of means. Means that share the same letter indicate non-significant differences ($P \leq 0.05$).
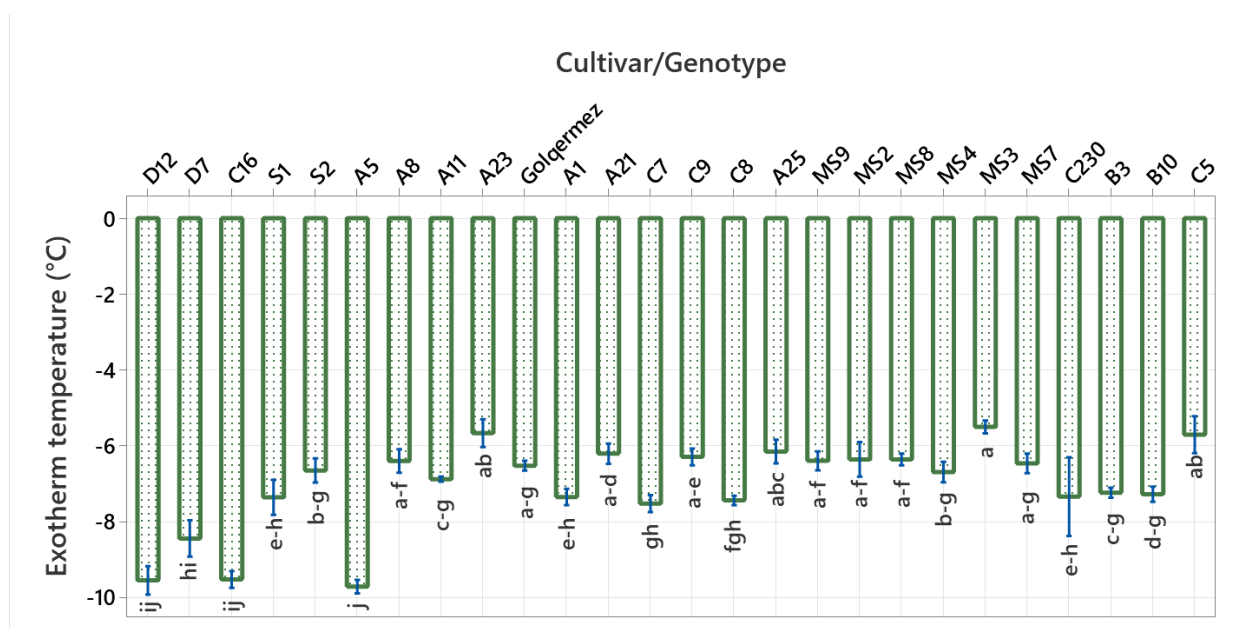

Fig. 14. Exotherm temperature of almond leaf buds sampled at the green leaf tip visible stage in 2019. Vertical bars are the standard deviation (SD) of means. Means that share the same letter indicate non-significant differences ($P \leq 0.05$)

Frost damage

In 2019, A25, C9, Golqermez, and MS7 exhibited the highest percentages of frost damage to the flower buds, with 100%, 100%, 100%, and 91.65%, respectively. In 2020, SH6, Sahand, Marcona, and KD11 also experienced significant frost damage, with 100%, 100%, 84.44%, and 84.23%, respectively. In contrast, D12, A5, and A23 had the lowest frost damage percentages in 2019, with 38.33%, 41.11%, and 53.63%, respectively. In 2020, Saba, KD101, KD99, and D12 showed the lowest frost damage to the flower buds, with 36.87%, 40.91%, 44.54%, and 44.55%, respectively (Figs. 16 and 17).
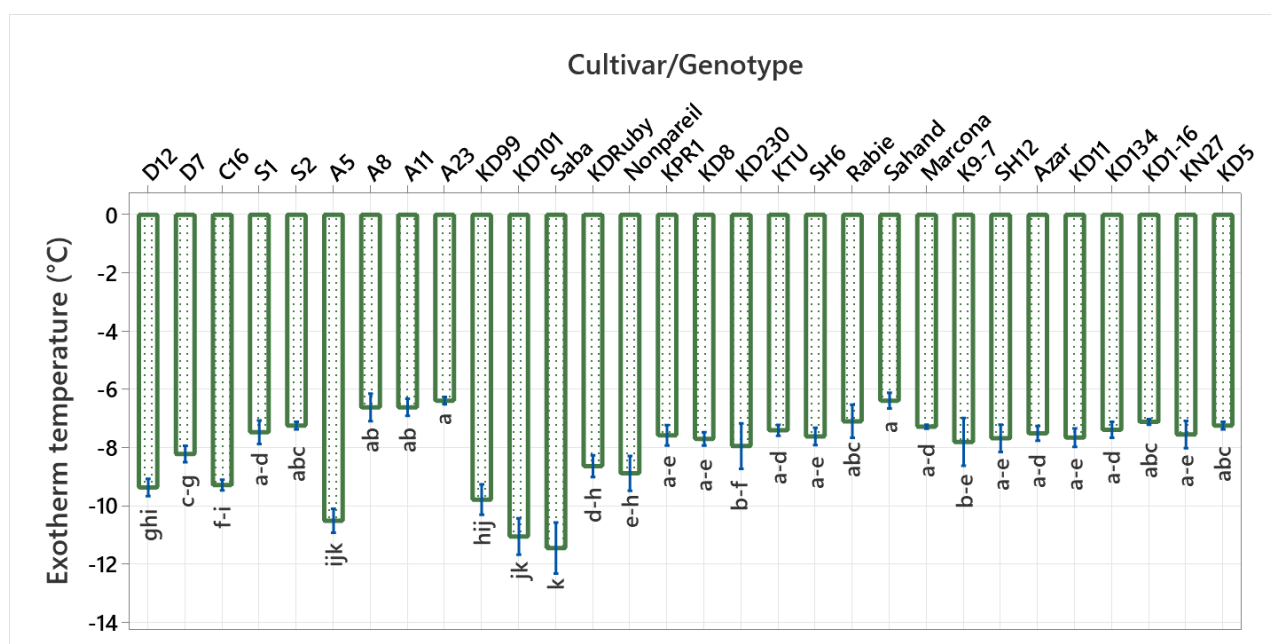
Fig. 15. Exotherm temperature of almond leaf buds sampled at the green leaf tip visible stage in 2020. Vertical bars show the standard deviation (SD) of means. Means that share the same letter indicate non-significant differences ($P \leq$ 0.05).
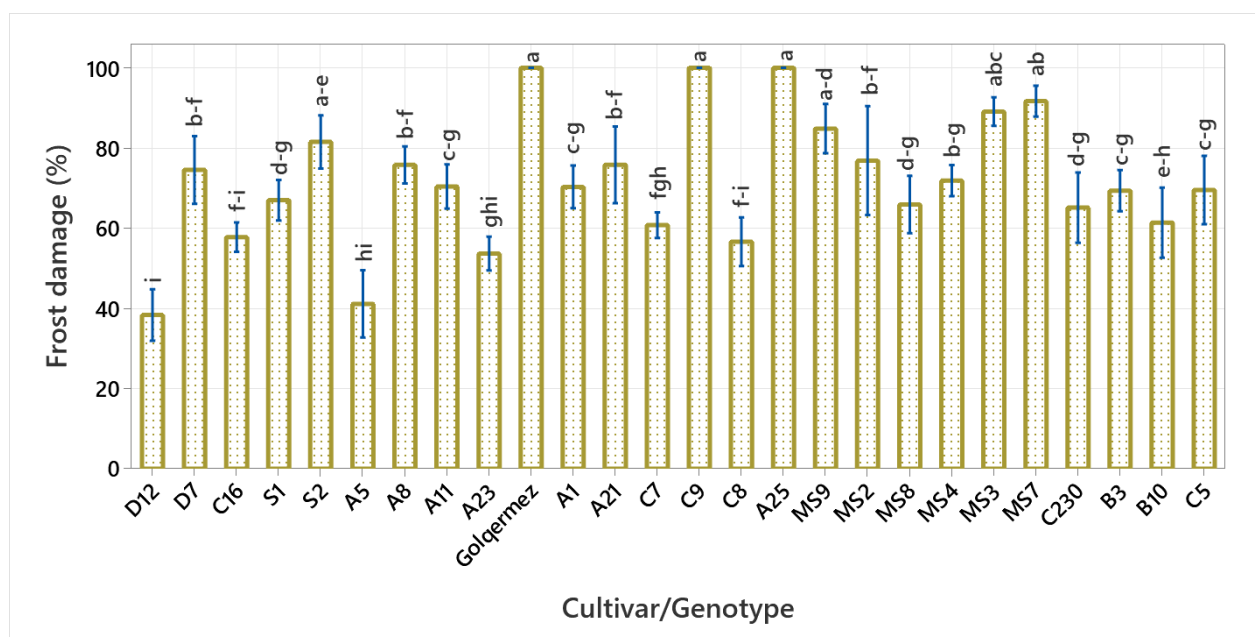

Fig. 16. Frost damage percentage of almond flower buds sampled at the open flower stage in 2019. Vertical bars are the standard deviation (SD) of means. Means that share the same letter indicate non-significant differences ($P \leq$ 0.05).

Ion leakage

In 2019, the cultivars/genotypes with the highest ion leakage percentages were MS8 (56.68%), A25 (56.31%), MS4 (55.73%), Golqermez (54.94%), C9 (54.54%), S1 (54.22%), MS3 (53.27%), and S2 (52.83%). In 2020, the cultivars/genotypes with the highest ion leakage percentages were SH6 (64.15%), Marcona (63.12%), and K9-7 (60.44%). On the other hand, the cultivars/genotypes with the lowest ion leakage percentages were D12 (39.12%), A5 (40.51%), and C16 (43.91%) in 2019, and KD99 (38.94%), Saba (40.06%), and D12 (40.45%) in 2020 (Figs. 18 and 19).
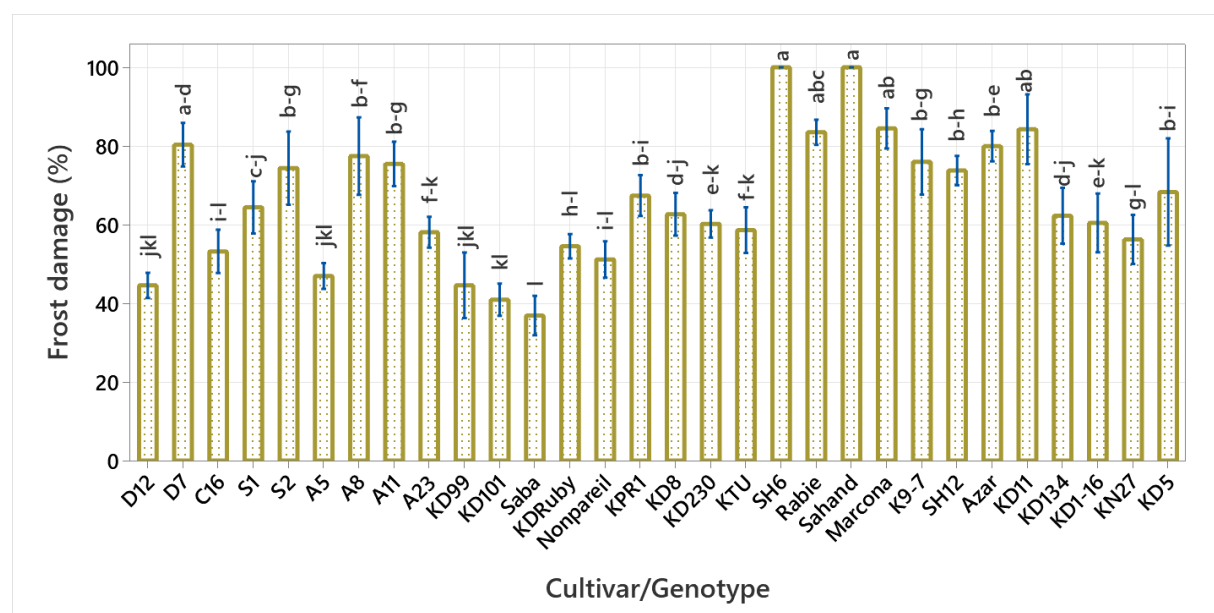
Fig. 17. Frost damage percentage of almond flower buds sampled at the open flower stage in 2020. Vertical bars represent the standard deviation (SD) of means. Means that share the same letter indicate non-significant differences ($P \leq 0.05$).

Fig. 18. Ion leakage percentage of almond flower buds sampled at the open flower stage in 2019. Vertical bars denote the standard deviation (SD) of means. Means that share the same letter indicate non-significant differences ($P \leq 0.05$).
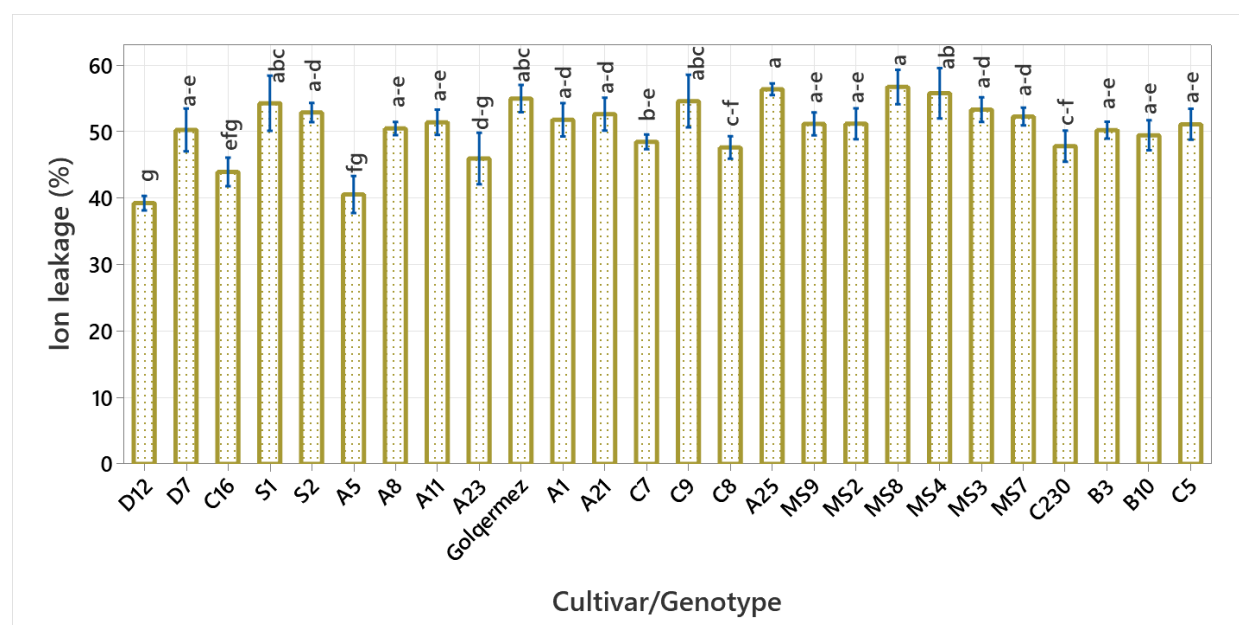
Correlations between the variables of the second experiment

Our study revealed a strong correlation between the temperature at which the leaf buds begin to freeze (LBET) and the temperature at which the flower buds begin to freeze (FBET) in both 2019 (r = 0.896, p = 0.000) and 2020 (r = 0.907, p = 0.000). Additionally, significant positive correlations were observed between both LBET and FBET with frost damage and ion leakage in 2019 and 2020 (Figs. 20 and 21).

Fig. 19. Ion leakage percentage of almond flower buds sampled at the open flower stage in 2020. Vertical bars show the standard deviation (SD) of means. Means that share the same letter indicate non-significant differences ($P \leq$ 0.05).

Fig. 20. Matrix plot of the correlations between leaf bud exotherm temperature (LBET), flower bud exotherm temperature (FBET), frost damage, and ion leakage from almond buds sampled in 2019 (r: Pearson's correlation coefficient, n = 26).

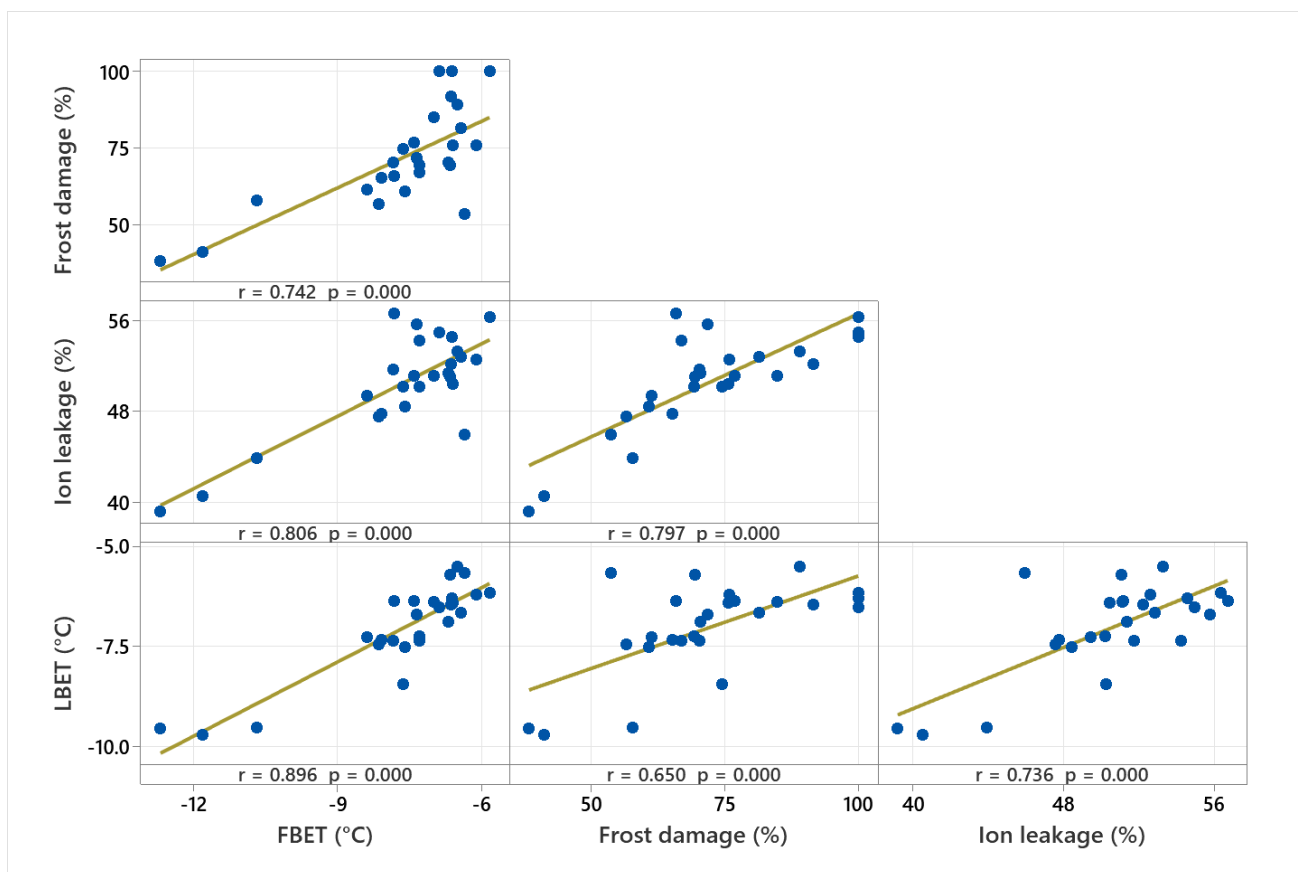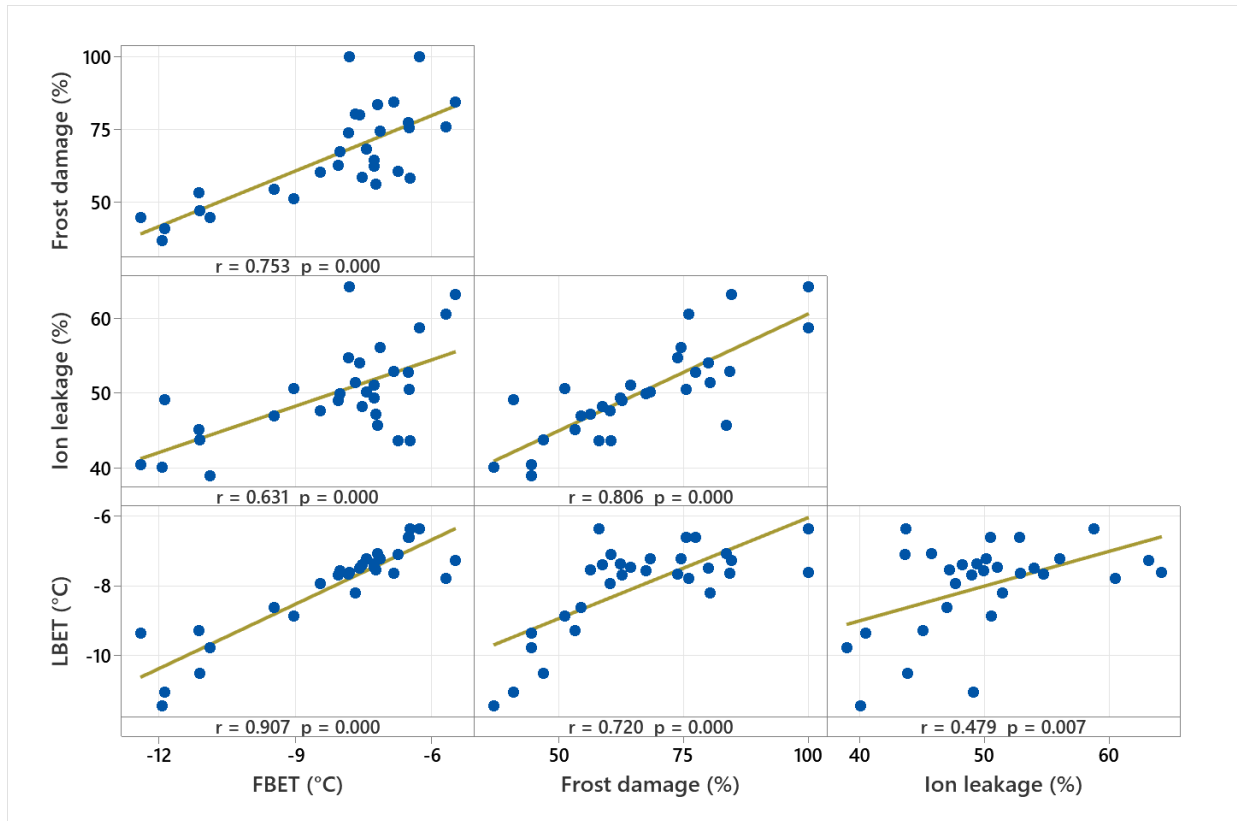**Fig. 21.** Matrix plot of the correlations between leaf bud exotherm temperature (LBET), flower bud exotherm temperature (FBET), frost damage, and ion leakage from almond buds sampled in 2020 (r: Pearson's correlation coefficient, n = 30).

Discussion

During the controlled freezing and thermal analysis of plant tissues, time-temperature profiles often reveal one or more exotherms. The first exotherm, known as the High-Temperature Exotherm (HTE), is associated with the formation of extracellular ice. The last observable exotherm, the Low-Temperature Exotherm (LTE), marks the freezing of the remaining water within the protoplast (Faust, 1989). In our study, thermal analysis of flower and leaf buds consistently exhibited a single-peaked exotherm. Previous research supports this observation, showing that during the bud break phase, differential thermal analysis detects a single-peaked exotherm in the flower buds of deciduous species such as apricot, sweet cherry, sour cherry, peach, plum, nectarine, pear, apple, and quince (Kaya et al., 2020; Kaya et al., 2018; Meng et al., 2007). For almond buds, a single-peaked exotherm may indicate simultaneous freezing of intracellular and extracellular compartments. This phenomenon is attributed to the xylem vessels' integrity between the shoot and the bud, which is established during the bud break phase. This connection causes the buds to lose their deep supercooling capacity (Kaya and Kose, 2022).

Ice propagation begins immediately upon the re-establishment of xylem integrity between the bud and the stem (Ashworth, 1984). As bud dormancy breaks, the flower buds of many deciduous species progressively lose their supercooling capacity, allowing ice to propagate into flower tissues (Rodrigo, 2000). Studies have confirmed that a single-peaked exotherm observed during controlled freezing is a reliable indicator for predicting the lethal temperature of buds (Kaya and Kose, 2022; Kaya et al., 2020; Kaya et al., 2018). During different growth stages, the highest exotherm temperature (-6.3 °C) was recorded at the green tip stage, which was higher than those observed during the popcorn (-7.97 °C) and open flower (-7.52 °C) stages. Additionally, the range of exotherm temperatures at the green tip stage (-5.21 °C for A23 to -6.77 °C for S2) was narrower compared to those at the popcorn (-6.81 °C for A23 to -12.27 °C for A5) and open flower (-6.35 °C for A23 to -11.81 °C for A5) stages.

It is important to note that the exotherm temperature at the green tip stage may not represent the buds' lethal temperature or be

suitable for evaluating the spring frost tolerance of various almond cultivars and genotypes. Similar results have been reported for sweet cherry cultivars, where higher exotherm temperatures were observed at the side green, green tip, and open cluster stages compared to the first white and full bloom stages (Kaya and Kose, 2022). Previous studies have identified a logarithmic relationship between the fresh weight of samples and their exotherm temperatures, suggesting that the use of small tissue samples might overestimate super-cooling in intact plants (Andrews et al., 1986; Ashworth and Davis, 1984). However, our study found no significant correlation between fresh weight and bud exotherm temperature. Additionally, the area under the curve (AUC), which reflects the heat of crystallization and is influenced by the bud's fresh weight and moisture content, also showed no significant correlation with bud exotherm temperatures.

Thus, it was concluded that exotherm temperatures at the three phenological stages (green tip, popcorn, and open flower) were not affected by the fresh weight of the buds. Instead, these temperatures are likely influenced by other factors, including phenological, physiological, and biochemical attributes such as organic acid and sugar compositions, which vary by genotype and cultivar (Kaya et al., 2021; Rodrigo, 2000).

In 2019 and 2020, the exotherm temperatures of almond flower buds at the open flower stage and almond leaf buds at the green leaf tip visible stage varied significantly among different cultivars and genotypes. These variations were directly correlated with frost damage, indicating that thermal analysis is a valuable tool for assessing frost tolerance in almond genotypes and cultivars. Similarly, previous thermal analysis studies have reported significant differences in the exotherm temperatures of flower buds across various apricot and sweet cherry cultivars (Kaya and Kose, 2022; Kaya et al., 2018).

Our research revealed a strong correlation between the exotherm temperature of flower buds at the open flower stage and that of leaf buds at the green leaf tip visible stage. This suggests that the factors influencing the exotherm temperatures of flower buds are likely similar to those affecting leaf buds. These findings have important implications for almond tree physiology and open avenues for future research, particularly regarding the potential of using thermal analysis of leaf buds as an early indicator of cold tolerance in almond seedlings before they reach the flowering phase.

Frost damage affects plant cell membranes by reducing their permeability and increasing their susceptibility to breakage, leading to solute leakage from damaged cells. Measuring ion leakage is a widely used method in plant cold tolerance research (Barranco et al., 2005; Lindén et al., 2000). In our study, we observed significant differences in ion leakage among various almond genotypes and cultivars in 2019 and 2020. This response positively correlated with frost damage and exotherm temperatures, suggesting that ion leakage could serve as a practical and reliable indicator for evaluating frost tolerance in almonds. Consistent with previous studies, more frost-resistant cultivars and genotypes exhibited lower ion leakage (Imani et al., 2011).

Based on thermal analysis, the cultivars and genotypes D12, Saba, KD101, KD99, A5, and C16 have been identified as top candidates for future almond breeding programs. These selections can serve as valuable genetic resources for further investigations into almond cold hardiness, particularly in regions prone to late spring frost damage. While the correlations between exotherm temperatures, frost damage, and ion leakage were strong, it is important to note that frost tolerance assessments in almond cultivars and genotypes may vary slightly depending on the measurement method employed. Therefore, further research is needed to validate the responses of different genotypes and cultivars to freezing temperatures using diverse methodologies. Evaluating the spring frost tolerance of almond cultivars and genotypes through thermal analysis will deepen our understanding of almond cold hardiness. This approach also facilitates the efficient utilization of almond genetic resources, which holds significant scientific and economic importance for regions facing challenges from late spring frost damage.

Conclusions
The first experiment revealed that the phenological stage and genotype significantly influenced the exotherm temperature of almond flower buds. This variation was not correlated with the fresh weight of the buds, indicating that other physiological and biochemical factors are responsible. An intriguing question arose from the finding that the exotherm temperature at the green tip stage was higher than at the popcorn and open flower stages. This observation highlights the need for further studies to understand the underlying mechanisms. In the second experiment, the correlations between the exotherm temperatures of flower and leaf buds, frost damage, and ion leakage were analyzed. The results demonstrated that thermal analysis is a practical tool for evaluating cold tolerance in

almonds. Specifically, assessing the frost tolerance of almond cultivars and genotypes through the thermal analysis of leaf buds at the green leaf tip visible stage confirmed the patterns of flower bud damage observed at the open flower stage. To validate these findings, additional research involving field studies with almond cultivars and genotypes that are resistant or susceptible to low temperatures is necessary. Furthermore, investigating physiological and biochemical factors related to spring frost tolerance—such as organic acids, sugar content, proline levels, and other variables—could provide deeper insights. Studying the correlations between these variables and the exotherm temperatures of flower and leaf buds across different phenological stages would also be highly beneficial.

Conflict of Interest
The authors indicate no conflict of interest in this work.

References
Andrews PK, Proebsting EL, Gross DC. 1986. Ice nucleation and supercooling in freeze-sensitive peach and sweet cherry tissues. Journal of the American Society for Horticultural Science 111(2), 232-236. https://doi.org/10.21273/JASHS.111.2.232

Ashworth E, Davis G. 1984. Ice nucleation within peach trees. Journal of the American Society for Horticultural Science 109(2), 198-201. https://doi.org/10.21273/JASHS.109.2.198

Ashworth E, Lightner G, Rowse D. 1981. Evaluation of apricot flower bud hardiness using a computer-assisted method of thermal analysis. HortScience 16(6), 754-756. https://doi.org/10.21273/HORTSCI.16.6.754

Ashworth EN. 1984. Xylem development in Prunus flower buds and the relationship to deep supercooling. Plant Physiology 74(4), 862-865. https://doi.org/10.1104/pp.74.4.862

Aslamarz AA, Vahdati K, Rahemi M, Hassani D, Leslie C. 2010. Supercooling and cold-hardiness of acclimated and deacclimated buds and stems of Persian walnut cultivars and selections. HortScience 45(11), 1662-1667. https://doi.org/10.21273/HORTSCI.45.11.1662

Barranco D, Ruiz N, Gómez-del-Campo M. 2005. Frost tolerance of eight olive cultivars. HortScience 40(3), 558-560. https://doi.org/10.21273/hortsci.40.3.558

Bigdeli Moheb M, Imani A, Shamili M. 2018. The evaluation of almond progenies of cold-susceptible and cold-tolerant parents (Filippo-Ceo × Shahrood-12). Scientia Horticulturae 234, 176-183. https://doi.org/10.1016/j.scienta.2018.02.044

Faust M. 1989. Physiology of temperate zone fruit trees. Wiley. https://books.google.rs/books?id=nvDwAAAAMAAJ

Imani A, Barzegar K, Piripireivatlou S. 2011. Relationship between frost injury and ion leakage as an indicator of cold hardiness in 60 almond selections. Journal of Nuts 3(2), 29-36. https://doi.org/10.22034/jon.2011.515758

Imani A, Ezaddost M, Asgari F, Masoumi S, Raeisi I. 2012. Evaluation of almond resistance to frost in controlled and field conditions. Journal of Nuts 3(2), 29-36. https://doi.org/10.22034/jon.2012.515728

Imani A, Mahamadkhani Y. 2011. Characteristics of almond selections in relation to late frost spring. Journal of Nuts 3(2), 29-36. https://doi.org/10.22034/jon.2011.515754

Kang S, Motosugi H, Yonemori K, Sugiura A. 1998. Supercooling characteristics of some deciduous fruit trees as related to water movement within the bud. The Journal of Horticultural Science and Biotechnology 73(2), 165-172. https://doi.org/10.1080/14620316.1998.11510960

Kaya O, Kose C. 2019. Cell death point in flower organs of some apricot (Prunus armeniaca L.) cultivars at subzero temperatures. Scientia Horticulturae 249, 299-305. https://doi.org/10.1016/j.scienta.2019.01.018

Kaya O, Kose C. 2022. Sensitivity of some sweet cherry (Prunus avium L.) cultivars to late spring frosts during different phenological stages following bud burst. Theoretical and Applied Climatology 148(3), 1713-1725. https://doi.org/10.1007/s00704-022-04030-7

Kaya O, Kose C, Donderalp V, Gecim T, Taskın S. 2020. Last updates on cell death point, bud death time, and exothermic characteristics of flower buds for deciduous fruit species by using differential thermal analysis. Scientia Horticulturae 270, 109403. https://doi.org/10.1016/j.scienta.2020.109403

Kaya O, Kose C, Esıtken A, Turan M, Utku O. 2021. Can organic acid and sugar compositions be used to predict cell death point limits? Receptacle and pistil organs of apricot (Prunus armeniaca L.). Rendiconti Lincei. Scienze Fisiche e Naturali 32(3), 493-509. https://doi.org/10.1007/s12210-021-01007-y

Kaya O, Kose C, Gecim T. 2018. An exothermic process involved in the late spring frost injury to flower buds of some apricot cultivars (Prunus armeniaca L.). Scientia Horticulturae 241, 322-328.
https://doi.org/10.1016/j.scienta.2018.07.019

Lindén L, Palonen P, Lindén M. 2000. Relating freeze-induced electrolyte leakage measurements to lethal temperature in red raspberry. Journal of the American Society for Horticultural Science 125(4), 429-435. https://doi.org/10.21273/JASHS.125.4.429

Liu J, Lindstrom OM, Chavez DJ. 2019. Differential thermal analysis of 'Elberta' and 'Flavorich' peach flower buds to predict cold hardiness in Georgia. HortScience 54(4), 676-683. https://doi.org/10.21273/HORTSCI13518-18

Malyshev AV, Beil I, Kreyling J. 2020. Differential Thermal Analysis: A fast alternative to frost tolerance measurements. In: Hincha DK, Zuther E, editors. Plant Cold Acclimation: Methods and Protocols. Springer US. p. 23-31. https://doi.org/10.1007/978-1-0716-0660-5_3

MENG Q-r, LIANG Y-q, WANG W-f, DU S-h, LI Y-h, YANG J-m. 2007. Study on supercooling point and freezing point in floral organs of apricot. Agricultural Sciences in China 6(11), 1330-1335. https://doi.org/10.1016/S1671-2927(07)60180-1

Mills LJ, Ferguson JC, Keller M. 2006. Cold-hardiness evaluation of grapevine buds and cane tissues. American Journal of Enology and Viticulture 57(2), 194-200. https://doi.org/10.5344/ajev.2006.57.2.194

Miranda C, Santesteban LG, Royo JB. 2005. Variability in the relationship between frost temperature and injury level for some cultivated Prunus species. HortScience 40(2), 357-361. https://doi.org/10.21273/hortsci.40.2.357

Nazemi Z, Zeinolabedini M, Hallajian MT, Bouzari N, Majidian P, Ebrahimi MA. 2016. Assessment of Iranian apricot cultivars resistant, susceptible and mutant to late spring frost. https://doi.org/10.22058/jpmb.2016.25530

Pakkish Z, Tabatabaienia MS. 2016. The use and mechanism of NO to prevent frost damage to flower of apricot. Scientia Horticulturae 198, 318-325.
https://doi.org/10.1016/j.scienta.2015.12.004

Quamme HA. 1974. An exothermic process involved in the freezing injury to flower buds of several Prunus species. Journal of the American Society for Horticultural Science 99(4), 315-318. https://doi.org/10.21273/jashs.99.4.315

Rodrigo J. 2000. Spring frosts in deciduous fruit trees—morphological damage and flower hardiness. Scientia Horticulturae 85(3), 155-173. https://doi.org/10.1016/S0304-4238(99)00150-8

Salazar-Gutiérrez MR, Chaves B, Anothai J, Whiting M, Hoogenboom G. 2014. Variation in cold hardiness of sweet cherry flower buds through different phenological stages. Scientia Horticulturae 172, 161-167. https://doi.org/10.1016/j.scienta.2014.04.002

Socias i Company R, Gradziel TM. 2017. Almonds: Botany, production and uses. CABI. https://books.google.com/books?id=_FU7jgEACAAJ

Yu DJ, Lee HJ. 2020. Evaluation of freezing injury in temperate fruit trees. Horticulture, Environment, and Biotechnology 61, 787-794. https://doi.org/10.1007/s13580-020-00264-4